Solid oxide fuel cell redox instability characterized by *in situ* transmission electron microscopy

Center for Electron Nanoscopy

Q. Jeangros[a], A. Faes[a,b], J. B. Wagner[c], T. W. Hansen[c], R. Dunin-Borkowski[c], J. Van herle[b], A. Hessler-Wyser[a]

Introduction and objectives

A solid oxide fuel cell (SOFC) cogenerates heat and electricity with high efficiency. Electricity is produced by the electrochemical reaction of a fuel (H_2, CO, CH_4) and an oxidant gas (O_2, air). The SOFC standard design is based on a anode-supported electrolyte. The anode is composed of yttria-stabilized zirconia (YSZ) and nickel oxide (NiO). NiO is reduced *in situ* into metallic nickel during the first use of the fuel cell. Porosity is formed to compensate the volume shrinkage induced by the reduction from NiO to Ni (40 vol%).

The nickel catalyst may reoxidize due to different factors. Nickel volume expansion (70 vol%) is not accommodated completely by the internal porosity. Stress is produced in the YSZ backbone. The performances of the SOFC degrade due to the creation of cracks in the electrolyte. The reason behind the irreversible effect of a redox cycle on Ni-based anodes is subject to controversies. Research groups suggest that the expansion of Ni upon a redox cycle is either caused by the reorganization of nickel during reduction or by formation of porosity upon reoxidation.

Time resolved environmental transmission electron microscopy was used in this study to characterize *in situ* the reduction and reoxidation mechanisms of Ni-based anodes and thus understand the exact causes of this degradation mechanism.

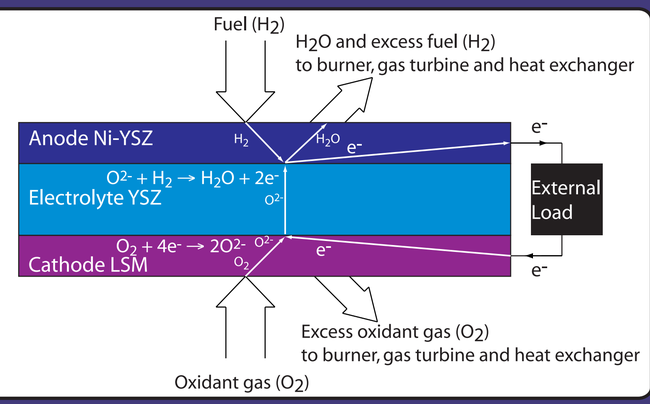

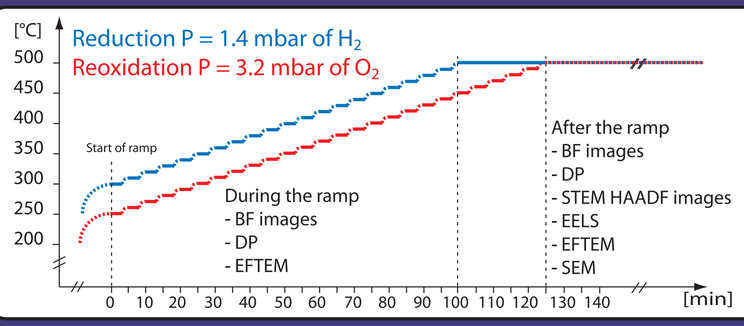

Experimental

TEM lamellas of 55 wt% NiO - 45 %wt YSZ anode were prepared by FIB lift-out method (stainless steel grid and platinum deposition).

The NiO-YSZ cermet was reduced *in situ* during a temperature ramp from 300°C to 500°C under a partial pressure of 1.4 mbar of H_2 in an environmental microscope FEI TITAN E-CELL™ at the Center for Electron Nanoscopy, Technical University of Denmark. Differential pumping apertures allow *in situ* S/TEM gas experiments to be performed.

The NiO-YSZ anode was then reoxidized *in situ* during a temperature ramp from 250°C to 500°C under a partial pressure of 3.2 mbar of O_2.

Bright field images (BF) and diffraction patterns (DP) were acquired in order to study the evolution of the micro/nanostructure and the crystallography as function of time and temperature.

Reduction

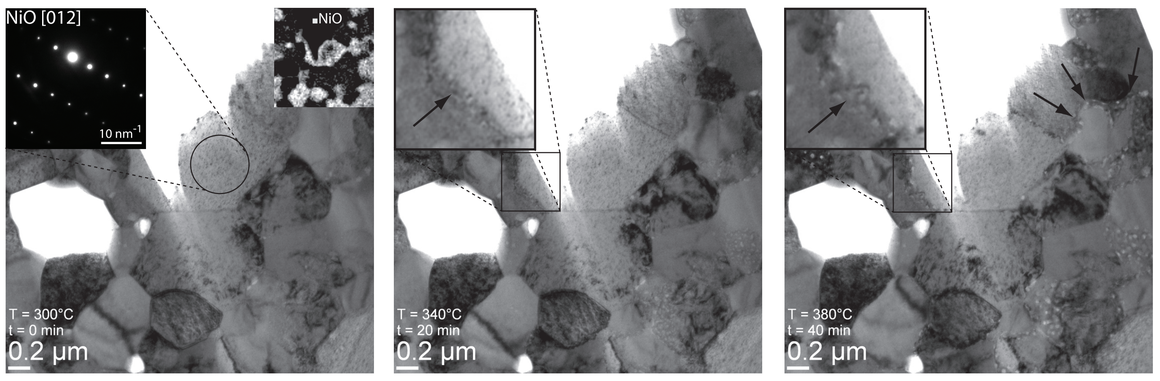

a) Initial as-sintered microstructure at the start of the in situ experiment under 1.4 mbar of H_2. The nickel EFTEM elemental map is in the top right corner.

b) Nanovoids start to appear at the NiO-YSZ interface to compensate the volume shrinkage induced by NiO reduction. YSZ acts as a transmitter of active species (hydrogen).

c) Nanoporosity grows towards the center of the grain. The creation of oxygen vacancies upon reduction enhances hydrogen adsorption on NiO.

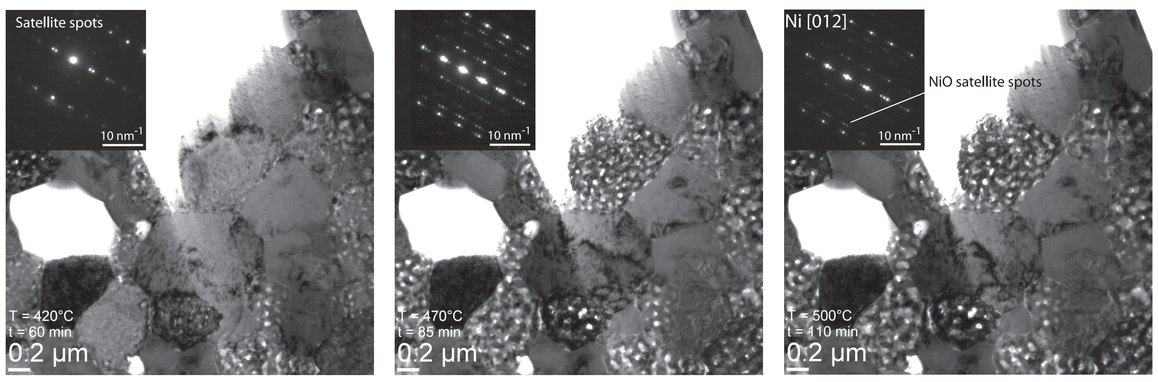

d) NiO free surface reduction starts to occur uniformly. A sufficient amount of surface oxygen vacancies is thermally generated to initiate the surface reduction. Satellite spots are observed in the diffraction pattern. Metallic nickel growth on its oxide is epitaxial.

e) Pores are now present on the surface of all nickel grains. The voids coalesce as the reduction continues.

f) Metallic Ni zone axis is the same as its oxide [012]. NiO satellite spots are still observed as the grains are not fully reduced.

Cross-section view of the TEM lamella
NiO-YSZ interface reduction
YSZ transmits active species to NiO

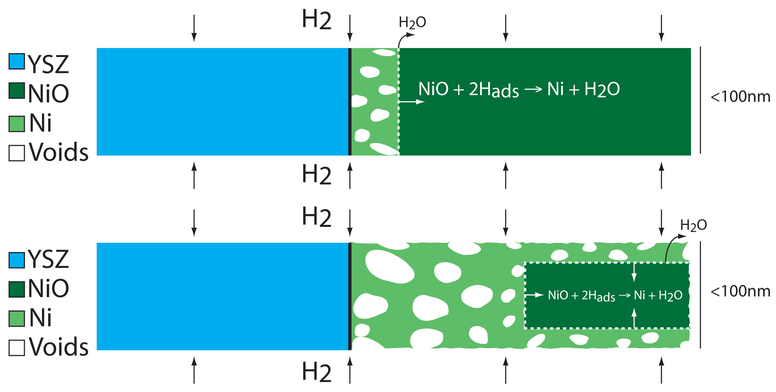

Free surface reduction
Surface oxygen vacancies initiate the free surface reduction

Reoxidation

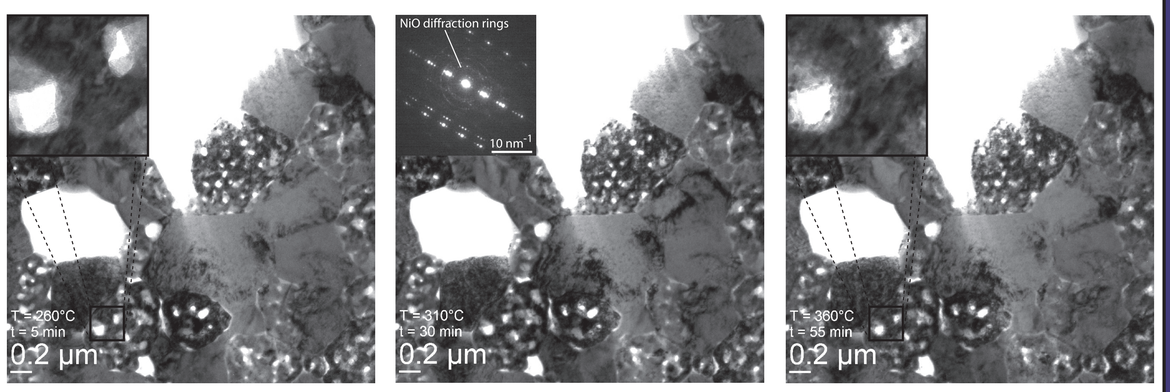

a) Reduced microstructure (metallic nickel) at the start of the *in situ* reoxidation under 3.2 mbar of O_2.

b) Diffraction rings start to appear. A polycrystalline NiO structure is created uniformly on the free surface.

c) The reoxidation continues. NiO slowly fills the intragranular porosity created during reduction. Nickel oxidation induces a volume expansion of 70%.

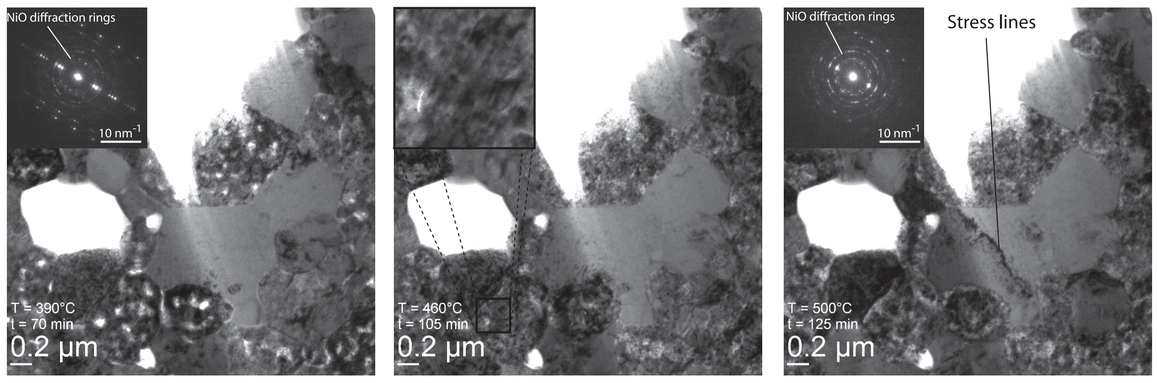

d) The surface reaction continues. Pores are filled by NiO crystallites.

e) The pores appear almost completely filled by the growth of NiO. The structure of the reoxidized grain is irregular.

f) Reoxidized NiO are porous. Bend contours underlining the presence of stress in the YSZ phase are observed.

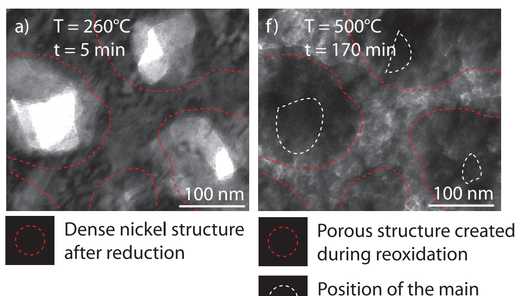

Dense nickel structure after reduction

Porous structure created during reoxidation

Position of the main porosity before reoxidation

Outward diffusion of Ni^{2+} through the oxide grain boundaries/dislocations is the dominant mass transport mechanism <1100°C.

Inward diffusion of O_2 through dynamically created and resealed fissures.

There is no balance between the two mechanisms: a porous reoxidized structure is created.

Nickel expands into as-sintered pores upon a redox cycle.

1) Growth of NiO crystallites
Accumulation of vacancies at the NiO/Ni interface as voids due to outward diffusion of Ni^{2+}

3) Compressive stress due to oxidation
Buckling of the NiO layer?
Local tensile stress caused by the new NiO?
Creation of a crack
Permeation of O_2 through the crack

4) NiO fills available space and crack
Vacancies injected at the NiO/Ni interface
Resealing of crack might be faster than void filling, porosity in NiO

5) Continuous formation and resealing of cracks
Porosity in the NiO
Coalescence of voids at the NiO/Ni interface
Porous structure, expansion upon a redox cycle

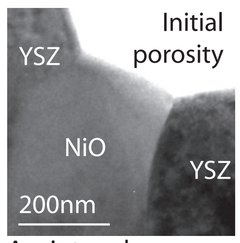

As sintered

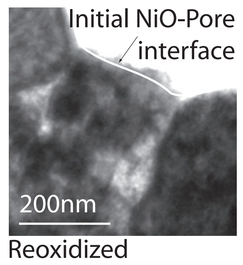

Reoxidized

Conclusion

In situ environmental transmission electron microscopy demonstrates the formation of internal porosity during reoxidation of the nickel catalyst. Intrinsic oxidation mechanisms create a porous reoxidized structure. Nickel expands upon a redox cycle. Internal porosity caused by NiO initial reduction does not totally accommodate the volume expansion induced by the reoxidation. Stress lines appear in the YSZ phase. Nickel sintering and coalescence during reduction was not observed.

[a] Interdisciplinary Center for Electron Microscopy (CIME), Ecole Polytechnique Federale de Lausanne (EPFL), CH-1015 Lausanne, Switzerland
[b] Laboratory of Industrial Energy Systems (LENI), EPFL, CH-1015 Lausanne, Switzerland
[c] Center for Electron Nanoscopy (CEN), Technical University of Denmark (DTU), DK-2800 Lyngby, Denmark

ÉCOLE POLYTECHNIQUE FÉDÉRALE DE LAUSANNE